

Mapping by Laser Photostimulation of Connections Between the Thalamic Reticular and Ventral Posterior Lateral Nuclei in the Rat

Ying-Wan Lam and S. Murray Sherman

Department of Neurobiology, Pharmacology and Physiology, University of Chicago, Chicago, Illinois

Submitted 25 February 2005; accepted in final form 1 June 2005

Lam, Ying-Wan and S. Murray Sherman. Mapping by laser photostimulation of connections between the thalamic reticular and ventral posterior lateral nuclei in the rat. *J Neurophysiol* 94: 2472–2483, 2005; doi:10.1152/jn.00206.2005. We used laser scanning photostimulation through a focused UV laser of caged glutamate in an *in vitro* slice preparation through the rat's somatosensory thalamus to study topography and connectivity between the thalamic reticular nucleus and ventral posterior lateral nucleus. This enabled us to focally stimulate the soma or dendrites of reticular neurons. We were thus able to confirm and extend previous observations based mainly on neuroanatomical pathway tracing techniques: the projections from the thalamic reticular nucleus to the ventral posterior lateral nucleus have precise topography. The reticular zone, which we refer to as a "footprint," within which photostimulation evoked inhibitory postsynaptic currents (IPSCs) in relay cells, was relatively small and oval, with the long axis being parallel to the border between the thalamic reticular nucleus and ventral posterior lateral nucleus. These evoked IPSCs were large, and by using appropriate GABA antagonists, we were able to show both GABA_A and GABA_B components. This suggests that photostimulation strongly activated reticular neurons. Finally, we were able to activate a disynaptic relay cell-to-reticular-to-relay cell pathway by evoking IPSCs in relay cells from photostimulation of the region surrounding a recorded relay cell. This, too, suggests strong responses of relay cells, responses strong enough to evoke spiking in their postsynaptic reticular targets. The regions of photostimulation for these disynaptic responses were much larger than the above-mentioned reticular footprints, and this suggests that reticulothalamic axon arbors are less widespread than thalamoreticular arbors, that there is more convergence in thalamoreticular connections than in reticulothalamic connections, or both.

INTRODUCTION

The thalamic reticular nucleus consists of a thin layer of GABAergic neurons that sits like a shield, mostly lateral to the thalamic relay nuclei. These inhibitory neurons are in a strategic position to regulate the communication between thalamus and cortex, because axons passing between the cortex and thalamus in both directions pass through the thalamic reticular nucleus and give off collaterals that innervate reticular neurons; the reticular neurons, in turn, provide a strong inhibitory input to relay cells (for reviews, see Jones 1985; Sherman and Guillery 2001). The issue addressed here concerns the functional nature of the topography between the thalamic reticular nucleus and the ventral posterior lateral nucleus, the latter being a first-order relay for somatosensory information (see Sherman and Guillery 2001).

The issue of topography is important, because it helps establish aspects of the function of the thalamic reticular

nucleus. Earlier reports have suggested that the thalamic reticular nucleus has rather diffuse connections with the relay nuclei (e.g., Jones 1975; Scheibel and Scheibel 1966; Steriade et al. 1993), but more recent evidence suggests that topography does exist, at least for parts of thalamus related to first-order relays (reviewed in Guillery and Harting 2003; Guillery et al. 1998). Evidence for topography has been anatomical, mostly using pathway tracing techniques (Guillery and Harting 2003; Guillery et al. 1998). In the ventral posterior lateral and medial nuclei of the rat, the axons of reticular neurons usually terminate in a compact arbor within a compact sphere, or more often, a short rod of tissue having its long axis oriented rostrocaudally. The diameters of these short rods were 100–150 μm and their length ranged between 250 and 300 μm (Cox et al. 1996; Pinault et al. 1995a,b). Cox et al. (1996) could differentiate two other termination patterns of reticular axons in younger animals: an intermediate arborization where the dimension of the branching structure was larger (585 by 359 μm) and a diffuse arborization with multiple arbors.

Evidence for topography in this projection to date has been anatomical, mostly using pathway tracing techniques (Guillery and Harting 2003; Guillery et al. 1998). The description for the topography between the thalamic reticular nucleus and the ventral posterior lateral nucleus is fairly typical in this regard (Crabtree 1992a,b, 1996). Here, the clearest evidence involves thin disks of reticular cells, oriented parallel to the border between the thalamic reticular and ventral posterior lateral nuclei. These disks and sites with which they connect were organized topographically in the direction perpendicular to the border in the horizontal sections of the brain; the topography in the direction parallel to the border is less well defined.

Our goal was to provide a mapping of the functional topography between the thalamic reticular and ventral posterior lateral nuclei to extend and clarify the mapping gleaned from pathway tracing studies. We did this using the technique of laser scanning photostimulation (Callaway and Katz 1993; Roerig and Chen 2002; Schubert et al. 2001; Shepherd et al. 2003) of *in vitro* slices through thalamus of the rat. We found a precise topography both parallel and perpendicular to the border between the thalamic reticular and ventral posterior lateral nuclei.

METHODS

Experiments were performed on thalamic slices taken from young rats (10–12 days postnatal). All animal procedures followed the animal care guidelines of the State University of New York.

Address for reprint requests and other correspondence: S. M. Sherman, Dept. of Neurobiology, Pharmacology and Physiology, Univ. of Chicago, Chicago, IL 60637 (E-mail: msherman@bsd.uchicago.edu).

The costs of publication of this article were defrayed in part by the payment of page charges. The article must therefore be hereby marked "advertisement" in accordance with 18 U.S.C. Section 1734 solely to indicate this fact.

Preparation of thalamic slices

To obtain the slices, each animal was deeply anesthetized by inhalation of isoflurane, and its brain was quickly removed and chilled in ice-cold artificial cerebrospinal fluid (ACSF), which contained (in mM) 125 NaCl, 3 KCl, 1.25 NaH_2PO_4 , 1 MgCl_2 , 2 CaCl_2 , 25 NaHCO_3 , and 25 glucose. Tissue slices were cut at 400 μm in the horizontal plane using a vibrating tissue slicer, transferred to a holding chamber containing oxygenated physiological saline maintained at 30°C, and incubated for ≥ 1 h before recording. Horizontal slices were used in our study because pathway tracing experiments (unpublished data) indicate that this plane of sectioning preserves most of the connections in both directions between the thalamic reticular and ventral posterior lateral nuclei.

Physiological recording

Whole cell recordings were performed using a visualized slice preparation as described previously (Lam et al. 2005). Recording pipettes were pulled from borosilicate glass capillaries and had tip resistances of 4–8 M Ω when filled with the appropriate solution. For most cells, this solution contained (in mM) 117 Cs-gluconate, 13 CsCl, 2 MgCl_2 , 10 HEPES, 2 $\text{Na}_2\text{-ATP}$, 0.3 Na-GTP, and 0.4% biocytin. In these cases, the K^+ channel blocker, Cs^+ , was included in the recording pipette to suppress $I_{\text{K-leak}}$ and help maintain the holding voltage at 0 mV. In some cells, we replaced the Cs^+ with K^+ or Na^+ (final concentration in mM: 135 K-gluconate, 7 NaCl, 2 MgCl_2 , 10 HEPES, 2 $\text{Na}_2\text{-ATP}$, 0.3 Na-GTP, and 0.4% biocytin) to test for the possibility of GABA_B responses, which require participation of K^+ channel activity. The pH of the intracellular solution was adjusted to 7.3 with CsOH (or KOH in cases where we avoided Cs^+) or gluconic acid, and the osmolality was 280–290 mOsm.

Recordings were obtained, often in pairs (see RESULTS), using an Axoclamp 2A amplifier in continuous single electrode voltage-clamp mode and an Axopatch 200B in voltage-clamp mode (Axon Instruments, Foster City, CA). The amplitudes of inhibitory postsynaptic currents (IPSCs) were maximized by holding the cells at 0 mV (Lam et al. 2005). The access resistance of the cells was constantly monitored throughout the recordings (>1 h each), and recordings were limited to neurons with a stable access of <30 M Ω throughout the whole experiment. Spontaneous IPSCs were usually not frequent enough to interfere with the experiments; in rare cases that they were, the recording was delayed until these spontaneous events subsided.

The GABA antagonists SR 95531 and CGP 46381 were purchased from Tocris (Ellisville, MO). All the other chemicals were purchased from Sigma-Aldrich (St. Louis, MO).

Photostimulation

Data acquisition and photostimulation were controlled by a program in Matlab (MathWorks, Natlick, MA) developed in the laboratory of Karel Svoboda (Shepherd et al. 2003), who generously shared this with us. Nitroindolyl (NI)-caged glutamate (Sigma-RBI; Canevari et al. 2001) was added to recirculating ACSF to a concentration of 0.39 mM during recording. Focal photolysis of the caged glutamate was accomplished by a pulsed UV laser (355 nm wavelength, frequency-tripled Nd:YVO₄, 100-kHz pulse repetition rate; DPSS Lasers, San Jose, CA). Figure 1A is a schematic illustration of the optics: the laser beam was directed into the side port of an Olympus microscope (BX50WI) using UV-enhanced aluminum mirrors (Thorlabs, Newton, NJ) and a pair of mirror galvanometers (Cambridge Technology, Cambridge, MA) and focused onto the brain slice with a low-magnification objective (4 \times 0.1 Plan, Olympus). Angles of the galvanometers were computer controlled and determined the position stimulated by the laser. The optics were designed to generate a nearly cylindrical beam in the slice so as to keep the mapping two dimensional (Shepherd et al. 2003). The Q-switch of the laser and a shutter (LS3-ZM2, Vincent Associate, Rochester, NY) controlled the timing of the laser. A variable neutral density wheel (Edmund, Barrington, NJ) attenuated the intensity of the laser to enable us to control the power of the laser at different levels during experiments. A thin microscope coverslip in the laser path reflected a small portion of the laser onto a photodiode. The current from this photodiode was amplified, acquired by the computer, and used to monitor the laser intensity throughout the experiment. During the setup and calibration of the optics, the laser powers corresponding to several levels of current output from the diodes were measured by a power meter (Thorlabs) at the back focal plane of the objectives. These data were used to plot a calibration curve, which in turn was used to provide the laser power estimates in this paper. Because the microscope objective blocks part of the laser path, we estimate that the power at the specimen is about 40% of that of the back focal plane.

Figure 1B is a photograph taken during a typical experiment. The borders between the internal capsule, thalamic reticular nucleus, and dorsal thalamus are indicated in this and other illustrations with dotted lines; thus the zone between dotted lines in each illustration represents

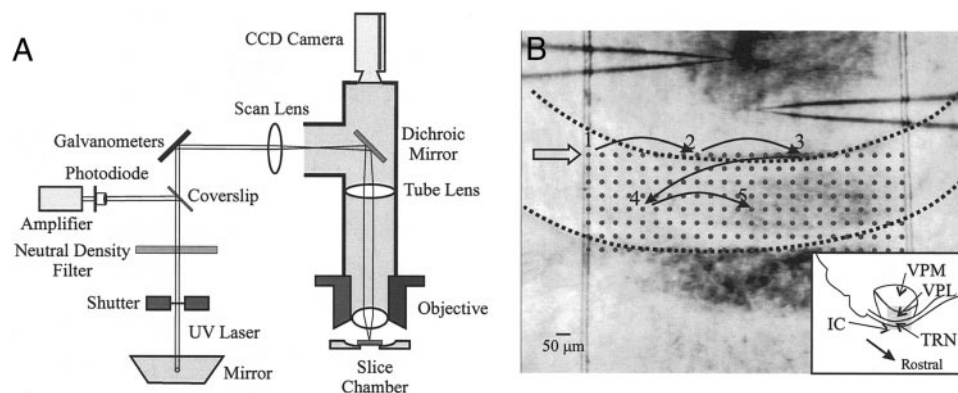


FIG. 1. Method for photostimulation. *A*: schematic diagram of the optics of the laser-scanning photostimulation setup used in this study. *B*: photomicrograph of recording preparation overlaid with a diagram of photostimulation sequence. Two recording pipettes are visible, and they are recording simultaneously from 2 cells in the ventral posterior lateral nucleus in a horizontal slice through the thalamus of the rat. Parallel, semitransparent bands (vertical in this view) seen in this and other photomicrographs are threads used to tether the slice. Each gray circle in the rectangular array indicates a location at which the laser is focused during the mapping trials. Spot locations are sampled in a distributed manner, and positions of the 1st 5 trials are indicated. Open arrow indicates origin used for overlaying photostimulation maps from different experiments (see Fig. 9). Dotted lines in this and other photomicrographs indicate the borders of the thalamic reticular nucleus, with the ventral posterior lateral above and the internal capsule below. Anatomical relationships here are shown schematically at a larger scale in the inset (VPM, ventral posterior medial nucleus; VPL, ventral posterior lateral nucleus; TRN, thalamic reticular nucleus; IC, internal capsule). Area shown in the photomicrograph is indicated by the gray rectangle.

the thalamic reticular nucleus. Brain slices were always placed at a similar angle inside the recording chamber to allow consistent comparison between experiments. A few threads of filaments, attached to a platinum wire slice holder, were used to tether the thalamic slices. The distance between these filaments was large (about 1 mm) relative to the recording configuration, and they were always carefully placed to avoid the area of recording and photostimulation (Fig. 1*B*) during experiments. We typically recorded from pairs of neurons in the ventral posterior lateral nucleus and mapped their inputs from the adjacent thalamic reticular nucleus with photostimulation in the latter nucleus. The standard stimulation pattern for mapping the reticular input consisted of 192 positions in a 24×8 array, with $50 \mu\text{m}$ between adjacent rows and columns (Fig. 1*B*, gray circles), and this covered about two-thirds to three-fourths of the thalamic reticular nucleus available in the slices. To avoid receptor desensitization, local caged-glutamate depletion, and toxicity, stimulation of these positions were arranged in a sequence that maximized the distance between consecutive trials (Fig. 1*B*). The light stimuli was 2 ms long, which consisted of 200 laser pulses. The time interval between photostimuli was 5 s. The laser power used (measured at the back-focal plane of the objective) ranged from 3 to 30 mW, but except for rare cases, it was <10 mW. If possible, multiple maps were done for a single pair with different laser powers to get a better estimate of the maximum extent of the thalamic reticular nucleus from which IPSCs were elicited. We did not see any change of the recording quality that suggested damage from the photostimulation.

In related experiments, the pathway from relay cells of the ventral posterior lateral nucleus to the thalamic reticular nucleus and back to the relay cells was studied by photostimulation of regions containing the recorded relay cell, using the same stimulation protocol as described above.

Data analysis

Responses were analyzed using programs written in Matlab. Pearson's correlations were calculated with Origin (Microcal, Northampton, MA). IPSCs evoked directly from the thalamic reticular nucleus were quantified by the total area under the traces (after being smoothed by 1-ms moving average) within 100 ms after laser stimulation. This was not appropriate for the disynaptic IPSCs evoked from photostimulation in the ventral posterior lateral nucleus, because this typically evoked a depolarization/IPSC sequence. Thus for these experiments, we measured the peak values of the evoked IPSCs. An equation similar to the calculation of the center of mass of a two-dimensional object was used to locate the centroid of the area of the thalamic reticular nucleus within which photostimulation elicited IPSCs.

$$\vec{M} = R_i \sum_i \vec{P}_i$$

where \vec{M} and \vec{P}_i are the coordinates of the centroid and stimulation positions, respectively, in vector form. R_i is the size of the IPSC response measured by the area under the curve or peak value of the smoothed traces. In nonvector form, the equation becomes

$$x_m = R_i \sum_i x_i$$

$$y_m = R_i \sum_i y_i$$

where (x_m, y_m) and (x_i, y_i) are the coordinates of the centroid and stimulation positions.

For presentation of the reticular input maps, traces of 150 ms recording immediately after the photostimulation were overlaid on top of a photomicrograph of the slice and pipettes (see RESULTS). Some of the photomicrographs were taken without using differential infrared-contrast (DIC) and brain regions including an extensive fiber representation, such as the internal capsule or ventral posterior lateral nucleus, thus appeared dark because of the high contrast settings of the video camera (e.g., Figs. 1, 6, and 7). The above-mentioned traces were arranged into a 24×8 array and placed where the laser was focused during the stimulation, so that the reticular area that projected to the recorded neuron could be visualized as that with a large upward current (IPSCs) in these traces. We refer to these afferent areas as "footprints." The centroid of the footprint is indicated in the figures with a red, blue, or black dot. Areas where the responses were $>20\%$ of the peak were interpolated using programs written in Matlab and surrounded by a red, blue, or black line. The reported areas of the resultant polygons were also calculated using Matlab. In cases where the polygons were too large and cut off, only the area inside the field of view was included. Differences in data (e.g., between the long and short axes of reticular footprints, areas of these footprints, and regions in which disynaptic relay cell-to-reticular-to-relay cell responses were elicited) were compared using a Student's *t*-test. The topographical arrangement of the reticular input was tested by calculating the Pearson correlation between the coordinates of the recording pipette and the centroid of the reticular footprint.

RESULTS

The data for these experiments are based on whole cell recordings from 68 neurons located sufficiently close to the

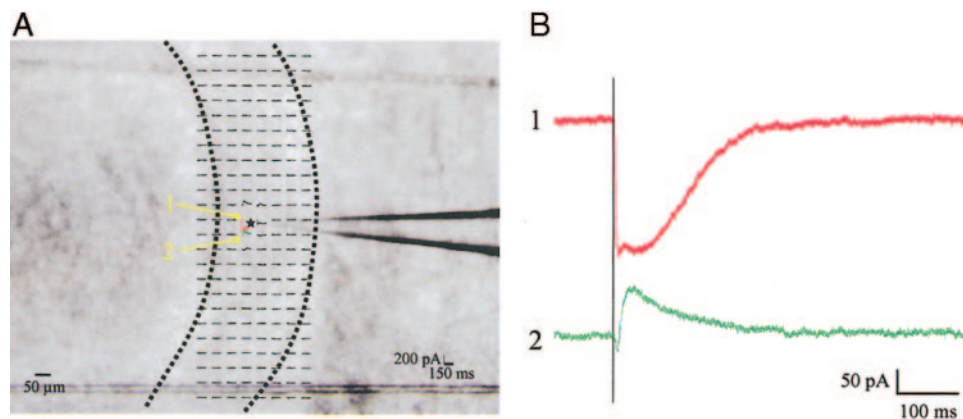


FIG. 2. Responses of a reticular neuron to direct photostimulation. *A*: responses of the neuron to photostimulation at 192 positions arranged in a 24×8 matrix. Responses were seen only in a narrow band of positions roughly parallel to the border between thalamic reticular nucleus and thalamus. Selected traces (color coded) are shown in *B* in a larger magnification. Ventral posterior lateral nucleus is located to the left of the dotted lines that indicate the location of the thalamic reticular nucleus. *B1*: photostimulation on the soma elicited direct depolarization (downward current) of the cell (red, top trace). *B2*: stimulation at positions slightly further away from the soma evoked a combination of an inhibitory postsynaptic current (IPSC; upward current) after an initial depolarization, being the small dip before the IPSC (green, bottom trace) in this cell. Laser power was 4 mW. Vertical line in *B* (and in the following illustrations) indicates the time of photostimulation.

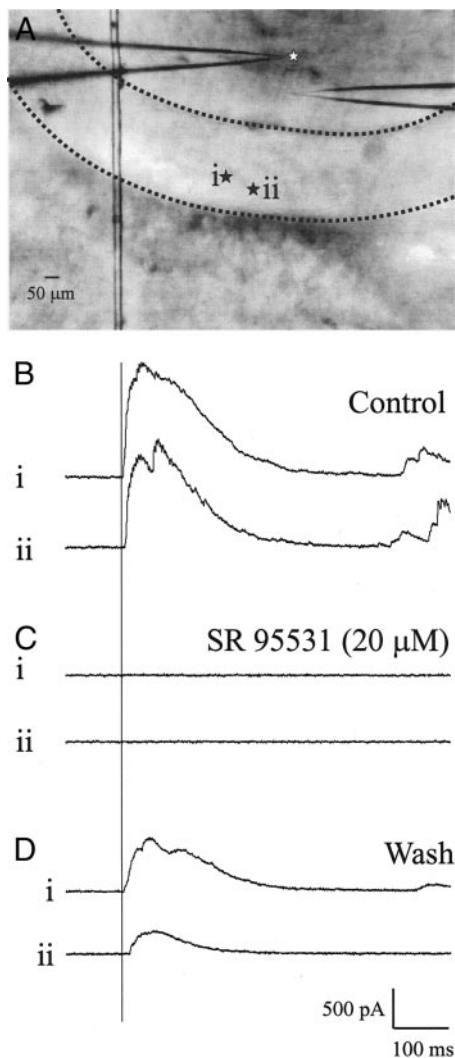


FIG. 3. Inhibitory postsynaptic currents (IPSCs) evoked by photostimulation (at 6 mW) of reticular cells are GABAergic. *A*: location of the relay cell (white star) and the 2 positions of photostimulation in the thalamic reticular nucleus (black stars, *i* and *ii*). *B*: top 2 traces are controls. *C*: evoked IPSC responses were abolished by the GABA_A antagonist, SR95531. *D*: responses recovered after the drug was washed out.

border with the thalamic reticular nucleus to be considered within the ventral posterior lateral nucleus. Of these, 26 pairs of relay cells were used to map the reticulothalamic pathway with photostimulation, and a subset of 25 (11 pairs and 3 singles) of these cells were used to study the thalamo-reticulothalamic pathway. In one experiment, photostimulation failed to evoke IPSCs in one of the cells. The data from this experiment were not included in the following quantitative analyses. The other 16 cells were used to study the effect of GABA antagonists and the response of reticular neurons to direct photostimulation.

Direct activation of neurons of the thalamic reticular nucleus

An example of the response of a reticular neuron to the direct photostimulation of the thalamic reticular nucleus, seen as an immediate inward current, is shown in Fig. 2. At the laser power used, the response to the photostimulation was evoked

only from a small area around the soma, and this was seen in all four reticular cells studied. In two of these cells, in addition to this direct response to stimulation near the soma (Fig. 2*B*, red, top trace), we also were able to evoke an additional outward current (or IPSC; Fig. 2*B*, green, bottom trace), but again, only from photostimulation near the soma. In none of the four reticular cells did we see any evidence of long-ranged synaptic or electrical connections that could compromise the spatial specificity of photostimulation.

Footprint of reticular input to ventral posterior lateral relay cells

Photostimulation in the thalamic reticular nucleus elicited large outward currents, or IPSCs, in recorded relay cells. Figure 3 shows that the evoked IPSCs are GABAergic, because they are blocked by the GABA_A antagonist SR95531, and this control was seen in five other cells tested for the direct reticulothalamic pathway. Finally, six cells were recorded without Cs⁺ in the electrode (see METHODS) to detect the possible presence of a GABA_B component to the IPSCs evoked

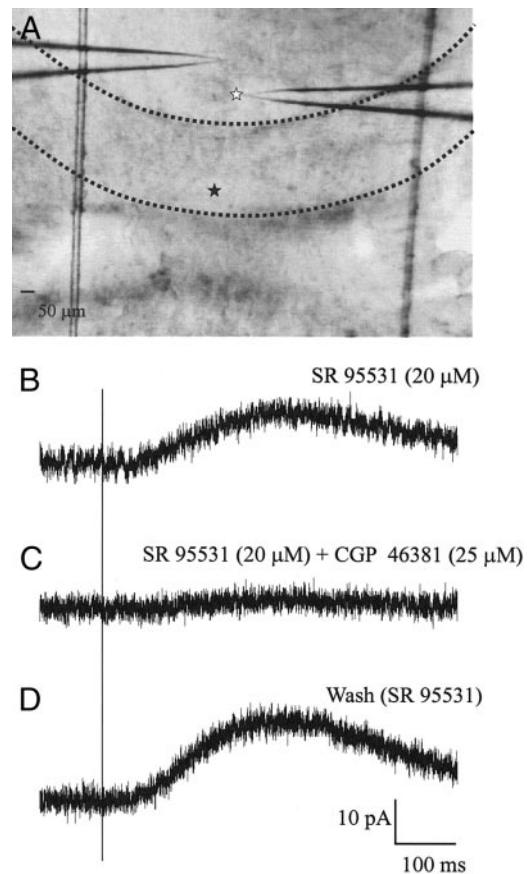


FIG. 4. GABA_B response in a relay cell of the ventral posterior lateral nucleus evoked by reticular photostimulation. The Cs⁺ in the intracellular solution was replaced by Na⁺ and K⁺, and the cell was held at -70 mV in these recordings. Laser power was 8 mW. All traces in *B*–*D* are averages of 6 responses to photostimulation in the same position within the thalamic reticular nucleus, with 5 s between each stimulation. *A*: photomicrograph taken during the recording. White star, location of the cell; black star, position of photostimulation. *B*: slow inhibitory current evoked by photostimulation during antagonism of GABA_A response by SR95531. *C*: remaining IPSC blocked by the specific GABA_B antagonist CGP46381. *D*: recovery of response after wash out of CGP46381.

by reticular photostimulation. As exemplified by Fig. 4, in each of these cells, we found evidence for such a response, because in the presence of the GABA_A antagonist SR95531, reticular photostimulation evoked long, slow IPSCs, with peaks of 25.1 ± 28.5 (SD) and a range of 2–80 pA that were reversibly blocked by the GABA_B antagonist, CGP46381.

With one exception among the 52 ventral posterior lateral relay cells for which we used photostimulation to map their reticular inputs, the reticular areas in which stimulation elicited IPSCs were elliptical in shape, with their long axes roughly parallel to the border between the thalamic reticular and ventral posterior lateral nuclei. We refer to each of these reticular areas of afferent input as a footprint. Figure 5 shows a typical example of the pattern commonly seen. The reticular input of

one ventral posterior lateral relay cell (indicated by the red star) was mapped by photostimulation at three different levels of laser output: 4 (Fig. 5A), 10 (Fig. 5C), and 40 mW (Fig. 5E). Each footprint is characterized by calculating a centroid (red dot) and a border determined by the level at which the response is 20% of the peak. Traces of selected pixels (marked by color) near the centroid are shown in Fig. 5, B, D, and F for clearer illustration of the evoked IPSC responses.

It is clear that photostimulation of only one small area of the thalamic reticular nucleus elicited IPSCs in the relay cells. As shown in this example, these IPSCs are large (>100 pA), even at the lowest power tested (Fig. 5B). We saw some IPSCs with long onset latencies (>100 ms; Fig. 5B, green traces, 2nd IPSC), which can be best interpreted as monosynaptic re-

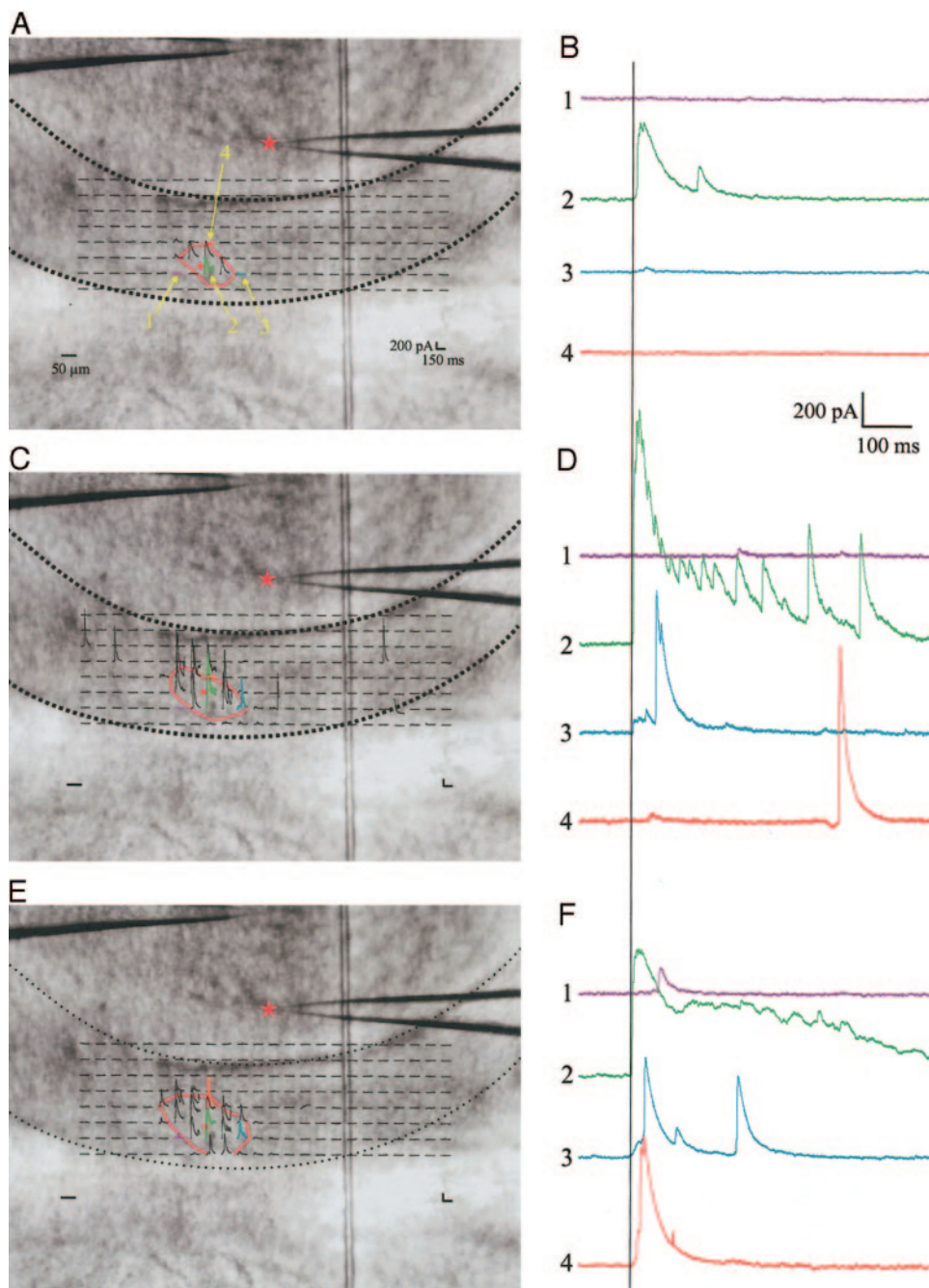


FIG. 5. Examples of responses to photostimulation and a "footprint" of thalamic reticular input to a thalamic relay cell (red star) in the ventral posterior lateral nucleus. Thalamic reticular nucleus was stimulated at the 3 laser powers of 4 (A), 10 (C), and 40 mW (E). Recordings for the 150 ms after photostimulation are overlaid on the photomicrograph at sites where the laser was focused (left column). The centroid of each response is indicated by a red dot. Area enclosing responses >20% of the peak response is indicated by a red line. Recordings in selected trials are shown in larger scale in the right column. A and B: responses evoked by photostimulation at laser power of 4 mW. Traces in B are color coded and further indicated by numbered arrows in A. B and D: responses evoked by photostimulation at laser power of 10 mW; conventions as in A and B. E and F: responses evoked by photostimulation at laser power of 40 mW; conventions as in A and B.

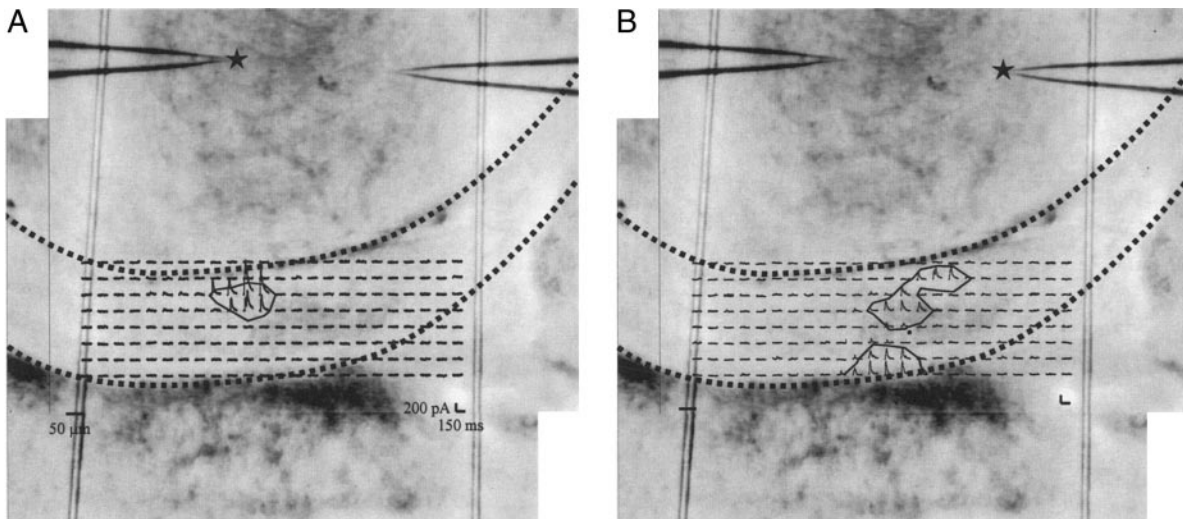


FIG. 6. Different reticular footprints of thalamic neurons. Two neurons were recorded in this experiment. *A*: footprint of 1 neuron (black star) with the usual single oval shape (black line). *B*: results from the other neuron (black star). This cell had 2 relatively large, nearby footprints. This was the only exception in the 52 experiments to the usual oval footprint.

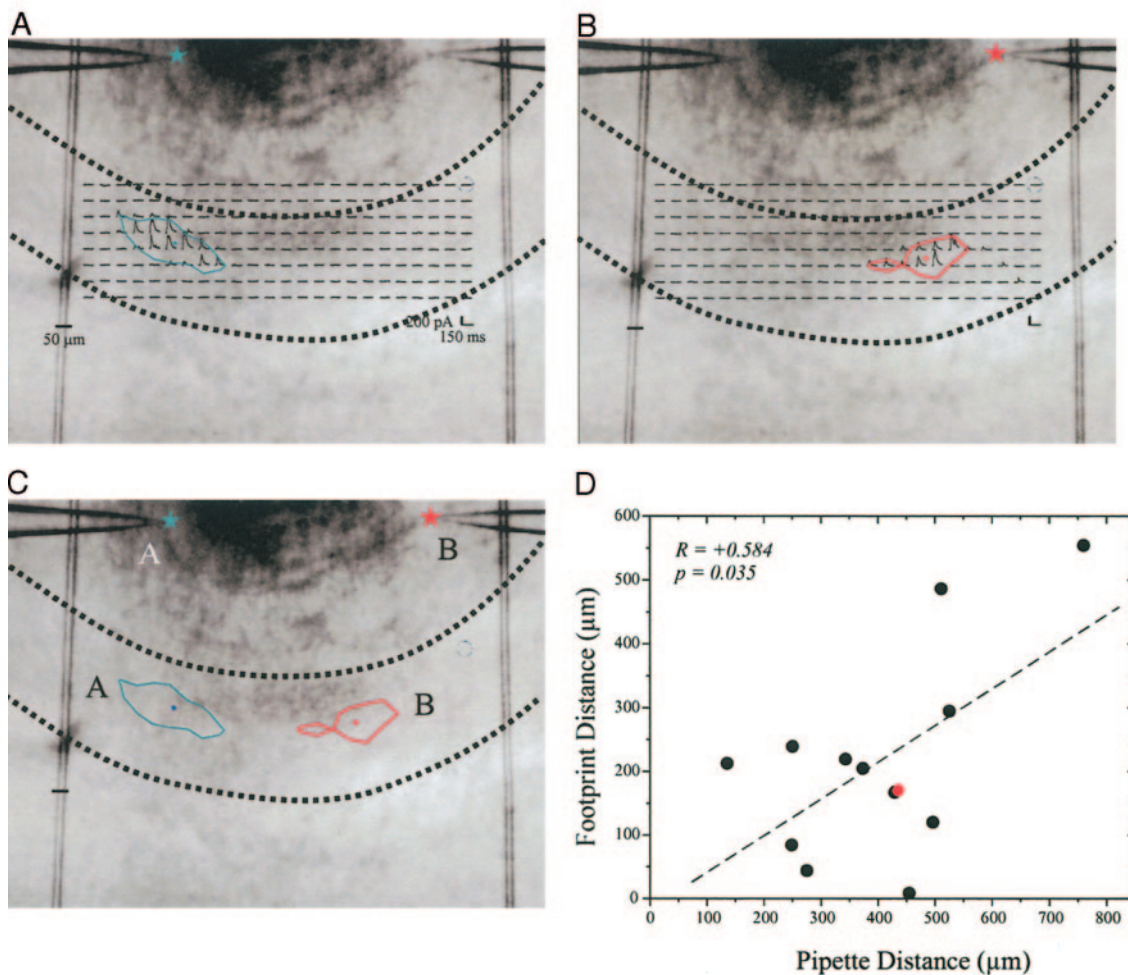


FIG. 7. Result from a pair of cells in the “horizontal” configuration; conventions for showing recordings, their sites, and photostimulation sites, with centroids, footprints, and the appropriate borders as in Fig. 2. The laser power was 5 mW. *A*: reticular footprint and recording for the 1st cell (blue star). *B*: results for the 2nd cell (red star). *C*: locations and extents of reticular footprints for both cells for comparison. *D*: plot of the horizontal distance between reticular footprint centroids vs. horizontal distance between pipettes in 13 paired-recording experiments. Red dot indicates result from the unusual experiment in Fig. 6*B*. Correlation ($R = +0.584$) is significant ($df = 12$; $P < 0.05$).

sponses to late spikes from the reticular neurons. Polysynaptic responses are unlikely, because the thalamic reticular nucleus consists only of GABAergic neurons, but these cannot be ruled out given the possibility that polysynaptic responses could involve some sort of postinhibitory rebound of postsynaptic reticular cells. The area of the reticular footprint increased with greater laser power (0.0138 mm² in Fig. 5A, 0.0244 mm² in Fig. 5C, and 0.0362 mm² in Fig. 5E), but the position of the centroid did not move significantly.

The only exception to the single elliptical footprint consisted of one neuron for which we saw two nearby footprints (see Fig. 6B). This result is included in our analyses and is shown separately as red circles in Figs. 7D and 9, B and C. In any case, exclusion of this pair of cells from the data set had no effect on the statistical evaluations.

The long and short axes of the oval stimulation footprints of the other 51 neurons were determined by eye and measured. The analyses gave an average length of $310 \pm 125 \mu\text{m}$ along the axis parallel to the border with the thalamic reticular nucleus and $117 \pm 37 \mu\text{m}$ along the axis approximately perpendicular to border. The average aspect ratio was 2.74 ± 1.13 , which is significantly different from the value representing a circular shape ($t = 11.17$, $df = 50$, $P < 0.0001$). The average footprint area was $0.024 \pm 0.012 \text{ mm}^2$.

The topographical relationship of the reticular inputs to the ventral posterior lateral relay cells was studied using simultaneous recordings of pairs of relay cells while photostimulation was applied to the thalamic reticular nucleus. These pairs were recorded in either a "horizontal" configuration, in which both cells were approximately equally distant from the border with the thalamic reticular nucleus (Fig. 7), or a "vertical" one, in which they were located along an axis perpendicular to this border (Fig. 8).

Figure 7 shows an example of the results from a pair of relay cells in the horizontal configuration. The response traces to photostimulation, the centroid, and extent of the input footprint for each member of the pair are shown in Fig. 7A (cell marked with blue star) and Fig. 7B (red star). Both footprints are shown in Fig. 7C for comparison. Figure 7D shows the horizontal separation between the two somata and the centroids of their reticular footprints and their relationships for all 13 pairs of cells studied in this fashion. We found a significant correlation between these measures ($r = +0.58$, $df = 12$, $P < 0.05$; Fig. 7D), indicating topography in the reticulothalamic pathway.

Figure 8 is an example of the recordings from a pair of cells in the vertical configuration. Results from the two cells are shown in Fig. 8, A (blue star) and B (red star), respectively. Their reticular inputs are shown together in Fig. 8C for comparison. Figure 8D

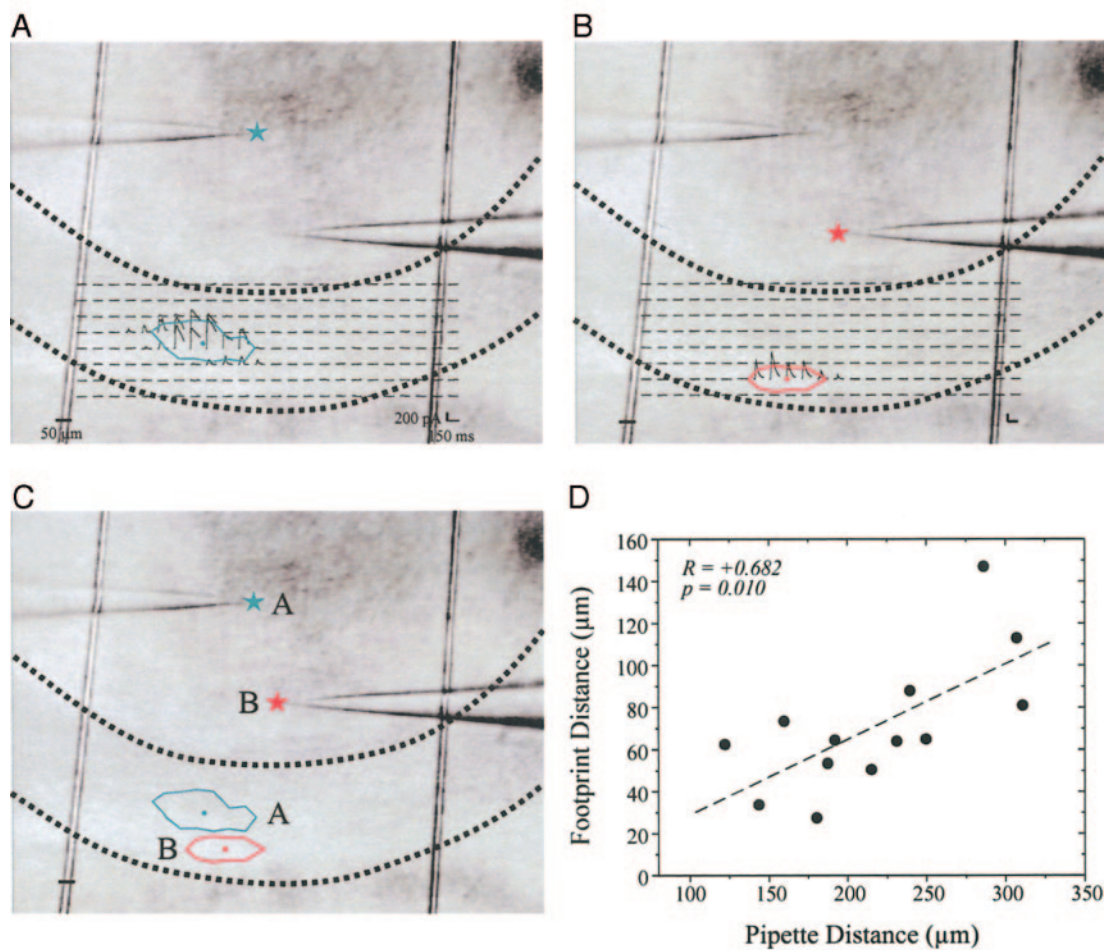


FIG. 8. Result from a pair of cells in the "vertical" configuration; other conventions as in Figs. 5 and 7; traces are overlaid where the laser was focused, and the centroid and 20% percent of peak are indicated. Laser power was 7 mW. A: reticular footprint and recording for the 1st cell (blue star). B: results for the 2nd cell (red star). C: locations and extents of reticular footprints for both cells for comparison. D: plot of the vertical distance between reticular footprint centroids vs. vertical distance between pipettes in 13 paired-recording experiments. The correlation ($R = +0.682$) is significant ($df = 12$; $P < 0.05$).

summarizes the correlation between the separation of the footprints and recorded cells for 13 pairs. The correlation is significant ($r = +0.68$, $df = 12$, $P < 0.05$, Fig. 8D), again indicating topography in the reticulothalamic pathway.

For comparison across experiments, the top left corner of the pattern of photostimulation in the thalamic reticular nucleus was assigned a coordinate (0,0); this is indicated by the gray open arrow in Fig. 1B and by the arrow and black star in Fig. 9A); the coordinates of the recorded ventral posterior lateral relay cells and the centroid of their reticular inputs were measured accordingly. These coordinates are plotted as connected circles in Fig. 9A; the exception in Fig. 6B is plotted as red triangles. A picture of one of the brain slices was overlaid in this relative plotting for reference; however, this is not precise because the dimensions and shapes varied from experiment to experiment. Figure 9B shows the correlation between the locations of the relay cells and their reticular inputs for the axis parallel to the reticular border, and Fig. 9C does the same for the axis perpendicular to this border. In both cases, the correlations are significant ($r = +0.52$, Fig. 9B; $r = +0.58$, Fig. 9C; $df = 51$, $P < 0.0001$ for both).

Pattern of relay cell-to-reticular-to-relay cell projections

As a supplement to the maps described above, we tried to establish the footprint of the inhibitory influence of ventral posterior lateral relay cells on their neighbors. Because there are virtually no interneurons in the rat ventral posterior lateral nucleus (Arcelli et al. 1997), we conclude that IPSCs evoked in recorded relay cells from photostimulation of their neighbors

results from a relay cell-to-reticular-to-relay cell pathway. In this fashion, we recorded the evoked IPSCs to neighborhood photostimulation for 25 relay cells in the ventral posterior lateral nucleus. For these recorded cells, we also determined the footprint in the thalamic reticular nucleus by photostimulation there as described above. Figure 10 shows examples of the data obtained. Photostimulation elicited an inward, depolarizing current in the area 50–100 μm around the recorded cell (Fig. 10, B, and D, purple and green traces), presumably because of direct photostimulation of the dendritic arbor of the recorded cell (the reversal potential of the glutamatergic currents was slightly more depolarized than the holding potential, 0 mV, in our recording). However, more interestingly, in all but one case, we saw IPSCs with longer delays riding on top of such direct depolarization (Fig. 10, B and D, green and blue traces). Moreover, IPSCs were typically (24 of 25 cells) elicited in a larger area around the cell, where direct depolarization from the photostimulation could not be detected (Fig. 10, B and D, blue traces). This we regard as the area from which nearby relay cells inhibit the recorded cell through the thalamic reticular nucleus. Our interpretation that this reflects activation of a disynaptic pathway means that photostimulation of the relay cells activates them strongly enough to create action potentials, and not just excitatory postsynaptic potentials (EPSPs), in their postsynaptic reticular targets.

Examples of the maps of these disynaptic responses from a pair are shown in Fig. 10, A and C. As in the cases in Figs. 5–8, recordings of the 150-ms period after the laser pulse are overlaid on top of the area of photostimulation. The area where the IPSCs were 20% of the peak was also interpolated and

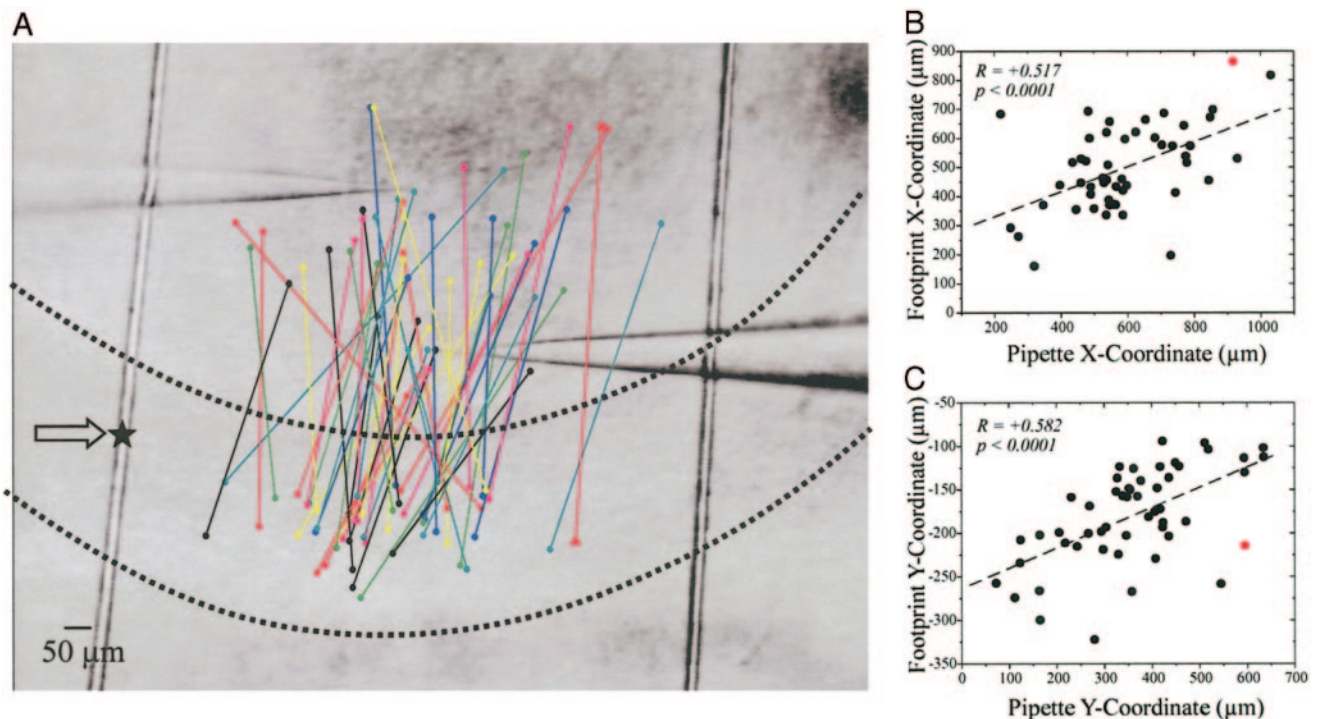


FIG. 9. Summary of results from all 52 cells. A: top left corner of the matrix of photostimulation locations (open arrow and star, see also Fig. 1B) was used as reference to calculate the coordinates of the cells and centroids of reticular footprints. These are plotted (in appropriate scale) here as connected color dots and are overlaid on top of the photomicrograph taken during 1 experiment to show approximate anatomical positions. Results from the unusual result in Fig. 6B is indicated with red triangles. B: abscissas of centroids plotted against those of recorded cells. Resulting correlation is significant ($R = +0.517$, $P < 0.0001$, $df = 51$). Red dot indicates cell in Fig. 6B. C: ordinates of centroids plotted against those of recorded cells. Resulting correlation is significant ($R = +0.582$, $P < 0.0001$, $df = 51$). Red dot indicates cell in Fig. 6B.

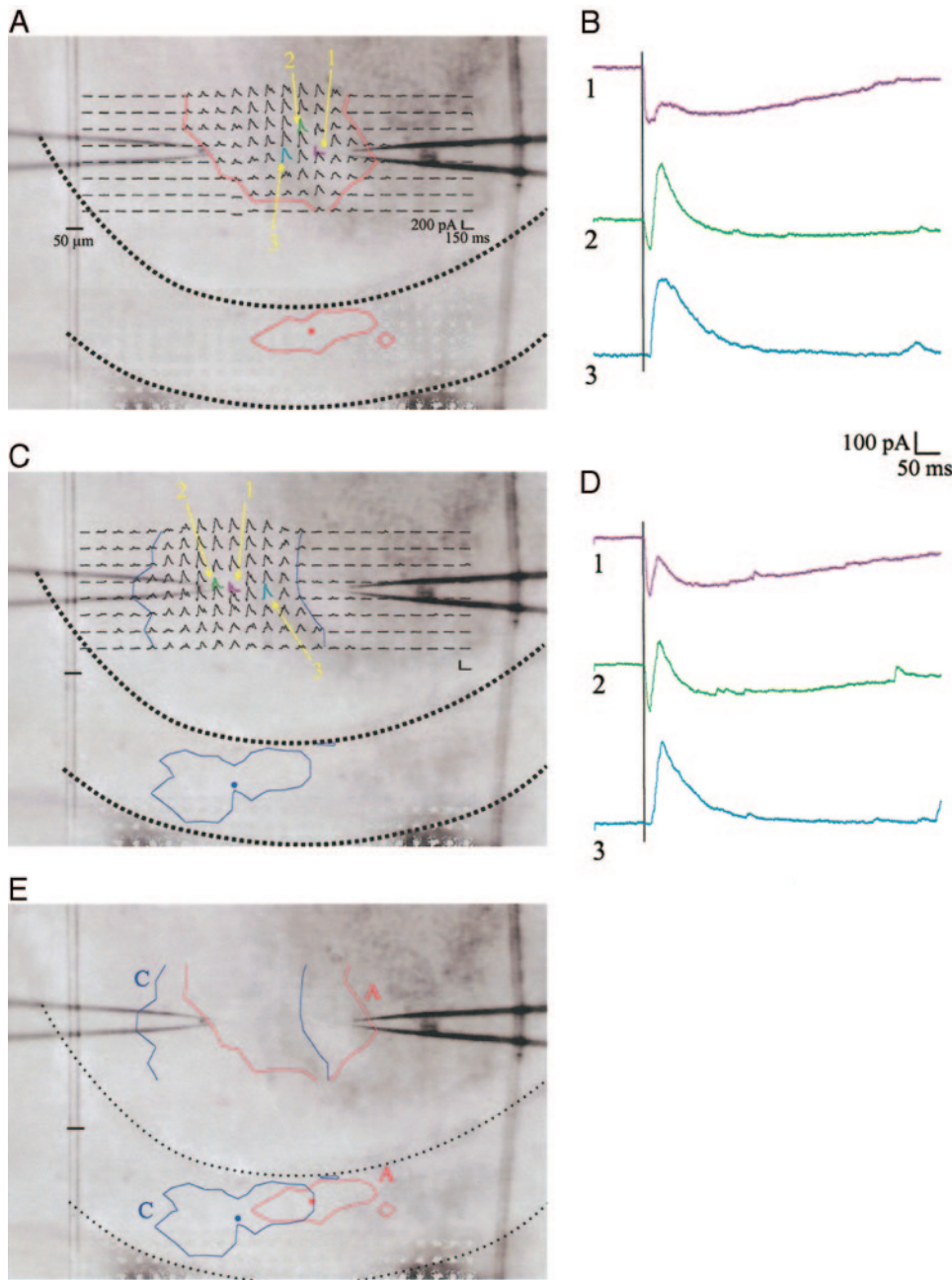


FIG. 10. Examples of disynaptic responses from photostimulation of the ventral posterior lateral nucleus along with reticular footprints as shown earlier. *A*: responses in 1 cell. Recordings for the period of 150 ms after the photostimulation are shown at each site of photostimulation. Borders within which the response is $>20\%$ of the peak are shown by red lines. Centroid and extent (20% peak) of reticular footprint, obtained separately, are also shown (red oval and centroid below). *B*: selected trials from *A* shown in larger scale with color coding. *C* and *D*: responses in 2nd cell; conventions as in *A* and *B* (except for blue lines being used). *E*: results from both cells are combined for comparison. Laser power used for mapping disynaptic responses was 9 mW; footprints were 5 mW.

indicated by red (Fig. 10*A*) or blue (Fig. 10*C*) lines. The reticular footprints mapped before were also shown for reference. Recordings of selected trials are indicated with colors and shown in expanded scale in Fig. 10, *B* and *D*. In Fig. 10*E*, both maps are combined for comparison, indicating that disynaptic responses could be elicited from a relatively large area around the recorded neurons. The average area calculated from these 24 experiments was $0.081 \pm 0.036 \text{ mm}^2$. This reported value is likely to be an underestimate, because in some cases, the area was cut off at the edge of the field of view of the camera. Nonetheless, this average area was significantly larger than the average reticular footprint area ($t = 10.04$, $df = 74$, $P < 0.0001$). The difference cannot be explained by different laser powers being used, because in 15 experiments, the same difference is found even when a similar laser power was used

in mapping both responses (data not shown). Figure 10*E* also shows that these two cells receive input from different, although overlapping, regions of the thalamic reticular nucleus. Figure 11 shows in another pair that these disynaptic responses are GABAergic, because they are blocked by the GABA_A antagonist SR95531, and this control was repeated for four other neurons.

DISCUSSION

We used photostimulation to confirm and extend with functional measures earlier anatomical evidence for topography in the connections between the thalamic reticular nucleus and the ventral posterior lateral nucleus (reviewed in Guillery and Harting 2003; Guillery et al. 1998). We found that, in the

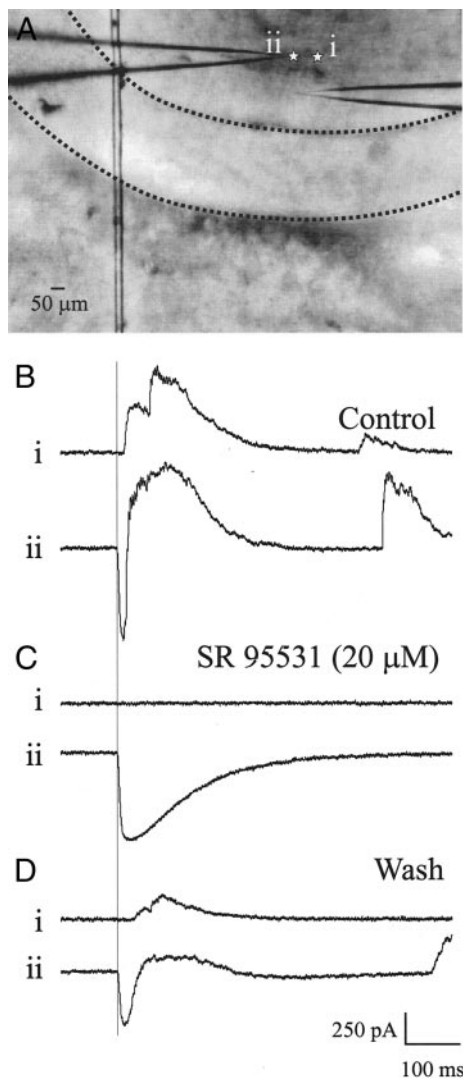


FIG. 11. Disynaptic responses of the thalamic neuron to adjacent photostimulation in the ventral posterior lateral nucleus are GABAergic. *A*: photomicrograph indicating the location of recording and photostimulation. The cell was stimulated at its soma (*ii*) or at an adjacent position (*i*). *B*: control for which somatic photostimulation evoked either large IPSC (*i*) or IPSCs riding on top of direct depolarization (*ii*). *C*: IPSCs inhibited by GABA_A antagonist SR95531 (middle pair of traces). *D*: recovery of response after SR95531 was washed out (bottom traces).

horizontal slice, the topography was clear in both mediolateral and anteroposterior directions (Fig. 9). However, these footprints were oval with the long axis parallel to the border between the thalamic reticular and the ventral posterior lateral nuclei (Figs. 5, 7, and 8). This may reflect the fact that reticular cells have disk-shaped dendritic arbors, with the long axis running parallel to this border (Lübke 1993; Pinault et al. 1995a,b; Scheibel and Scheibel 1966; Yen et al. 1985), so that there may thus be more area in this dimension parallel to the border to photostimulate given reticular neurons.

Although there is anatomical evidence that some reticulothalamic axons form diffuse arbors (Cox et al. 1996), we found no such examples. Perhaps this is because any such diffusely projecting reticular cells form weak and unreliable connections (Cox et al. 1996) that are not readily detected with photostimulation. It has also been argued that such diffuse projections of

reticular cells existed only transiently in developing animal (Pinault 2004). Our data add little to this controversy, but it does show that, functionally, the reticular projection to ventral posterior lateral relay cells in rat is already predominately topographical even at ages as young as 10 days old.

We were also able, with photostimulation, to show both GABA_A and GABA_B components to the IPSCs evoked from reticular activation (Figs. 3 and 4), suggesting that the photostimulation strongly activates reticular cells. In general, photostimulation evokes responses that are quite similar to those evoked by electrical stimulation in paired recordings (e.g., Kim et al. 1997). We thus conclude that photostimulation can be a reliable method for specifically stimulating the soma and dendrites of a neuron without affecting axons en passage in complex brain regions.

In limited experiments, we were also able to show at least some local, inhibitory interconnections between reticular cells that appear to be synaptic, although we did not thoroughly study this feature. We did not find evidence of strong electrical coupling between reticular neurons (Landisman et al. 2002) perhaps because these synapses exist only between neurons within a limited distance (<40 µm; Long et al. 2004) that is below the resolution of our maps, and this suggests that such coupling that is present did not greatly affect our topographical results.

Functional significance

Our experiments testing the topography of the relay cell-to-reticular-to-relay cell pathway (e.g., Fig. 10) is interesting for at least two reasons beyond the simple demonstration of topography. First, as noted in the RESULTS, our data indicate that photostimulation of relay cells must activate them sufficiently that they produce firing in the postsynaptic reticular neurons. This is consistent with evidence both that EPSPs generated in reticular cells from relay cells of the ventral posterior lateral nucleus are relatively large with a low failure rate (Gentet and

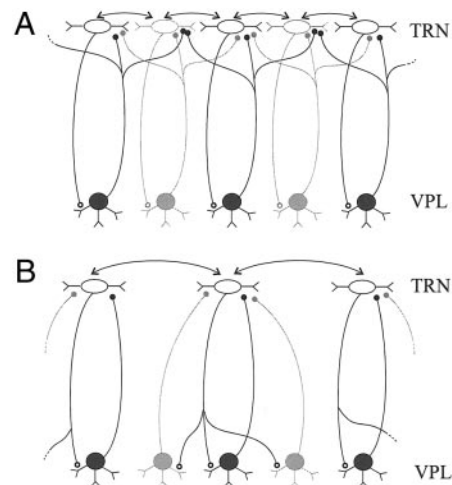


FIG. 12. Schematic illustrations of 2 possible patterns of connectivity between the thalamic reticular nucleus and the ventral posterior lateral nucleus that can explain our results. *A*: scheme in which reticulothalamic axon arbors are more restricted than thalamoreticular arbors. *B*: scheme in which there is larger convergence in thalamoreticular pathway than in reticulothalamic pathway. Coupling of reticular neurons by chemical and electrical synapses is indicated by double arrows.

Ulrich 2003, 2004) and that terminals from these relay cells are relatively large and proximally located on reticular cell dendrites (Liu and Jones 1999; Ohara and Lieberman 1981, 1985). In the parlance of Sherman and Guillery (1998), these observations suggest that relay cell inputs to these reticular cells are drivers, rather than modulators, meaning that these inputs convey the main information that is represented by the receptive fields of reticular cells.

Second, the zones of the ventral posterior lateral nucleus within which photostimulation evokes disynaptic IPSCs in relay cells are clearly larger than the footprints for monosynaptic photostimulation in the thalamic reticular nucleus; they are also considerably larger than the extent of the dendritic arbors of the relay cells (identified by a direct depolarizing response to photostimulation as in Fig. 10, *B* and *D*; detailed analysis not shown). As just noted, relay cells tend to innervate reticular cells proximally. There are two connectivity patterns suggested by Fig. 12 that could account for this; note that a combination of these patterns is also possible. (Chemical and electrical synapses between reticular neurons will be not discussed in detail, because they are beyond the scope of the reported results, but they are suggested here by double-headed arrows.) One (Fig. 12*A*) is that there is more spatial spread among thalamoreticular axon arbors than among reticulothalamic ones. The other (Fig. 12*B*) is related to the fact that there are more relay than reticular cells: this proposes that a spread of relay cells converges onto each reticular cell. Note that both circuits require relatively little convergence in the reticulothalamic projection, which is suggested by the small reticulothalamic footprints seen with photostimulation. While there is substantial anatomical evidence for restricted reticulothalamic arbors (Cox et al. 1996; Pinault and Deschênes 1998; Uhlrich et al. 1991), thalamoreticular arbors, which typically emanate as very thin collaterals of the thalamocortical axons, tend to be difficult to label completely, and thus the anatomical correlate we suggest has not yet been adequately resolved.

In summary, the thalamic reticular nucleus has long been thought to play a key role in thalamocortical information flow because of its strategic positions astride both thalamocortical and corticothalamic axons and also because of its inhibitory, GABAergic projection to relay cells. Just how reticular circuitry works to control thalamic relay functions has been the subject of some debate, partly because of the controversy surrounding both the specificity of reticulothalamic connections and also of the pattern of connections within the thalamic reticular nucleus itself. Our data indicate a precise topography to the reticulothalamic connections, supporting much previous anatomical evidence. These observation indicate that the thalamic reticular nucleus can regulate thalamocortical communication in a finely tuned and specific manner.

Our data also indicate local synaptic connections between reticular cells as well as a surprisingly strong pathway providing inhibition through the thalamic reticular nucleus from relay cells to neighboring relay cells. Thus the thalamic reticular nucleus could provide a mechanism of lateral inhibition between relay cells that serves to sharpen sensory processing through the thalamus.

ACKNOWLEDGMENTS

We thank G. Shepherd and K. Svoboda for allowing us to clone their laser scanning photostimulation microscope and software.

GRANTS

This research was supported by National Eye Institute Grant EY-03038 to S. M. Sherman and funding from the Howard Hughes Medical Institute to K. Svoboda.

REFERENCES

- Arcelli P, Frassoni C, Regondi MC, De Biasi S, and Spreafico R.** GABAergic neurons in mammalian thalamus: a marker of thalamic complexity? *Brain Res Bull* 42: 27–37, 1997.
- Callaway EM and Katz LC.** Photostimulation using caged glutamate reveals functional circuitry in living brain slices. *Proc Natl Acad Sci USA* 90: 7661–7665, 1993.
- Canepari M, Nelson L, Papageorgiou G, Corrie JE, and Ogden D.** Photochemical and pharmacological evaluation of 7-nitroindolyl- and 4-methoxy-7-nitroindolyl-amino acids as novel, fast caged neurotransmitters. *J Neurosci Meth* 112: 29–42, 2001.
- Cox CL, Huguenard JR, and Prince DA.** Heterogeneous axonal arborizations of rat thalamic reticular neurons in the ventrobasal nucleus. *J Comp Neurol* 366: 416–430, 1996.
- Crabtree JW.** The somatotopic organization within the cat's thalamic reticular nucleus. *Eur J Neurosci* 4: 1352–1361, 1992a.
- Crabtree JW.** The somatotopic organization within the rabbit's thalamic reticular nucleus. *Eur J Neurosci* 4: 1343–1351, 1992b.
- Crabtree JW.** Organization in the somatosensory sector of the cat's thalamic reticular nucleus. *J Comp Neurol* 366: 207–222, 1996.
- Gentet LJ and Ulrich D.** Strong, reliable and precise synaptic connections between thalamic relay cells and neurones of the nucleus reticularis in juvenile rats. *J Physiol* 546: 801–811, 2003.
- Gentet LJ and Ulrich D.** Electrophysiological characterization of synaptic connections between layer VI cortical cells and neurons of the nucleus reticularis thalami in juvenile rats. *Eur J Neurosci* 19: 625–633, 2004.
- Guillery RW, Feig SL, and Lozsádi DA.** Paying attention to the thalamic reticular nucleus. *Trends Neurosci* 21: 28–32, 1998.
- Guillery RW and Harting JK.** Structure and connections of the thalamic reticular nucleus: advancing views over half a century. *J Comp Neurol* 463: 360–371, 2003.
- Jones EG.** Some aspects of the organization of the thalamic reticular complex. *J Comp Neurol* 162: 285–308, 1975.
- Jones EG.** *The Thalamus*. New York: Plenum Press, 1985.
- Kim U, Sanchez-Vives MV, and McCormick DA.** Functional dynamics of GABAergic inhibition in the thalamus. *Science* 278: 130–134, 1997.
- Lam YW, Cox CL, Varela C, and Sherman SM.** Morphological correlates of triadic circuitry in the lateral geniculate nucleus of cats and rats. *J Neurophysiol* 93: 748–757, 2005.
- Landisman CE, Long MA, Beierlein M, Deans MR, Paul DL, and Connors BW.** Electrical synapses in the thalamic reticular nucleus. *J Neurosci* 22: 1002–1009, 2002.
- Long MA, Landisman CE and Connors BW.** Small clusters of electrically coupled neurons generate synchronous rhythms in the thalamic reticular nucleus. *J Neurosci* 24: 341–349, 2004.
- Liu XB and Jones EG.** Predominance of corticothalamic synaptic inputs to thalamic reticular nucleus neurons in the rat. *J Comp Neurol* 414: 67–79, 1999.
- Lübke J.** Morphology of neurons in the thalamic reticular nucleus (TRN) of mammals as revealed by intracellular injections into fixed brain slices. *J Comp Neurol* 329: 458–471, 1993.
- Ohara PT and Lieberman AR.** Thalamic reticular nucleus: anatomical evidence that cortico-reticular axons establish monosynaptic contact with reticulo-geniculate projection cells. *Brain Res* 207: 153–156, 1981.
- Ohara PT and Lieberman AR.** The thalamic reticular nucleus of the adult rat: experimental anatomical studies. *J Neurocytol* 14: 365–411, 1985.
- Pinault D.** The thalamic reticular nucleus; structure, function and concept. *Brain Res. Rev.* 46: 1–31, 2004.
- Pinault D, Bourassa J, and Deschênes M.** Thalamic reticular input to the rat visual thalamus: a single fiber study using biocytin as an anterograde tracer. *Brain Res* 670: 147–152, 1995a.
- Pinault D, Bourassa J, and Deschênes M.** The axonal arborization of single thalamic reticular neurons in the somatosensory thalamus of the rat. *Eur J Neurosci* 7: 31–40, 1995b.

- Pinault D and Deschênes M.** Projection and innervation patterns of individual thalamic reticular axons in the thalamus of the adult rat: a three-dimensional, graphic, and morphometric analysis. *J Comp Neurol* 391: 180–203, 1998.
- Roerig B and Chen B.** Relationships of local inhibitory and excitatory circuits to orientation preference maps in ferret visual cortex. *Cerebral Cortex* 12: 187–198, 2002.
- Scheibel ME and Scheibel AB.** The organization of the nucleus reticularis thalami: a Golgi study. *Brain Res* 1: 43–62, 1966.
- Schubert D, Staiger JF, Cho N, Kotter R, Zilles K, and Luhmann HJ.** Layer-specific intracolumnar and transcolumar functional connectivity of layer V pyramidal cells in rat barrel cortex. *J Neurosci* 21: 3580–3592, 2001.
- Shepherd GM, Pologruto T A, and Svoboda K.** Circuit analysis of experience-dependent plasticity in the developing rat barrel cortex. *Neuron* 38: 277–289, 2003.
- Sherman SM and Guillery RW.** On the actions that one nerve cell can have on another: distinguishing “drivers” from “modulators”. *Proc Natl Acad Sci USA* 95: 7121–7126, 1998.
- Sherman SM and Guillery RW.** *Exploring the Thalamus*. San Diego: Academic Press, 2001.
- Steriade M, McCormick DA, and Sejnowski TJ.** Thalamocortical oscillations in the sleeping and aroused brain. *Science* 262: 679–685, 1993.
- Uhlich DJ, Cucchiaro JB, Humphrey AL, and Sherman SM.** Morphology and axonal projection patterns of individual neurons in the cat perigeniculate nucleus. *J Neurophysiol* 65: 1528–1541, 1991.
- Yen C-T, Conley M, and Jones EG.** Morphological and functional types of neurons in cat ventral posterior thalamic nucleus. *J Neurosci* 5: 1316–1338, 1985.